

# Can Supercooled Phase Transitions explain the Gravitational Wave Background observed by Pulsar Timing Arrays?

Peter Athron,<sup>1,\*</sup> Andrew Fowlie,<sup>2,†</sup> Chih-Ting Lu,<sup>1,‡</sup> Lachlan Morris,<sup>3,§</sup> Lei Wu,<sup>1,¶</sup> Zhongxiu Xu,<sup>1,\*\*</sup> and Yongcheng Wu<sup>1,††</sup>

<sup>1</sup>*Department of Physics and Institute of Theoretical Physics, Nanjing Normal University, Nanjing, 210023, China*

<sup>2</sup>*Department of Physics, School of Mathematics and Physics,  
Xi'an Jiaotong-Liverpool University, Suzhou, 215123, China*

<sup>3</sup>*School of Physics and Astronomy, Monash University, Melbourne, Victoria 3800, Australia*

Several pulsar timing array collaborations recently reported evidence of a stochastic gravitational wave background (SGWB) at nHz frequencies. Whilst the SGWB could originate from the merger of supermassive black holes, it could be a signature of new physics near the 100 MeV scale. Supercooled first-order phase transitions that end at the 100 MeV scale are intriguing explanations, because they could connect the nHz signal to new physics at the electroweak scale or beyond. Here, however, we provide a clear demonstration that it is not simple to create a nHz signal from a supercooled phase transition, due to two crucial issues that should be checked in any proposed supercooled explanations. As an example, we use a model based on non-linearly realized electroweak symmetry that has been cited as evidence for a supercooled explanation. First, we show that a FOPT cannot complete for the required transition temperature of around 100 MeV. Such supercooling implies a period of vacuum domination that hinders bubble percolation and transition completion. Second, we show that even if completion is not required or if this constraint is evaded, the Universe typically reheats to the scale of any physics driving the FOPT. This redshifts the SGWB away from the required nHz range.

## I. INTRODUCTION

The North American Nanohertz Observatory for Gravitational Waves (NANOGrav) recently detected a stochastic gravitational wave background (SGWB) for the first time with a significance of about  $4\sigma$  [1]. This was corroborated by other pulsar timing array (PTA) experiments, including the Chinese Pulsar Timing Array (CPTA; [2]), the European Pulsar Timing Array (EPTA; [3]), and the Parkes Pulsar Timing Array (PPTA; [4]). Although the background could originate from mergers of super-massive black holes (SMBHs), this explanation might be inconsistent with previous estimates of merger density and remains a topic of debate [5–7]. Thus, there is an intriguing possibility that the SGWB detected by NANOGrav could originate from more exotic sources [8]. Indeed, many exotic explanations were proposed for an earlier hint of this signal [9, 10], including non-canonical kinetic terms [11], inflation [12–14], first-order phase transitions (FOPTs; [15, 16]), cosmic strings [17–20], axions and ALPs [16, 21–24], QCD [25], and dark sector models [26–31].

The nanohertz (nHz) frequency of the signal indicates that any new physics explanation should naturally lie at around 100 MeV. If there are new particles around the MeV scale there are constraints from cosmology [32–34] as any new particles must not significantly alter the number of relativistic degrees of freedom [35, 36], must not inject energy e.g. from

particle decays that could spoil big bang nucleosynthesis (BBN) and distort the cosmic microwave background (CMB), and must not lead to an overabundance of dark matter (DM). In any case, there are constraints from laboratory experiments, such as fixed-target experiments,  $B$ -factories and high-energy particle colliders. These constraints may weaken if the new particles are sequestered in a dark sector, though could be important if one wishes to connect the dark sector to the SM [37].

It is conceivable, however, that new physics at characteristic scales far beyond the MeV scale could be responsible for a nHz signal. This could happen, for example, if a FOPT (see Refs. [38–40] for reviews) starts at a temperature above the MeV scale but ends at the MeV scale due to supercooling. That is, the Universe remains in a false vacuum (a local minimum of the scalar potential) until the MeV scale because a transition to the true vacuum (the global minimum) is suppressed. This was previously considered in the context of the electroweak phase transition [41–48] and was discussed as a possible new physics explanation by NANOGrav [8, 10]. Supercooling could help new physics explanations evade constraints on MeV scale modifications to the SM and connect a nHz signal to new physics and phenomenology at the electroweak scale or above. For example, a scalar cubic coupling driving a supercooled FOPT [41] could be observable through the Higgs boson pair production at the Large Hadron Collider (LHC; [49]).

In this work, however, we raise two difficulties with supercooled FOPTs. We explicitly demonstrate that these difficulties rule out one of the earliest models that was constructed to explain a nHz GW signal through a supercooled FOPT [41]. This model was prominently cited as a viable example [8, 10]. The difficulties are that, firstly, supercooled FOPTs that reach nucleation may still struggle to complete [50] and requiring completion places stringent limits on the viable parameter space [51]. We show for the model proposed in Ref. [41] that requiring the phase transition completes places a lower bound on the transition temperature, or more precisely the

\*Electronic address: [peter.athron@njnu.edu.cn](mailto:peter.athron@njnu.edu.cn)

†Electronic address: [andrew.fowlie@xjtlu.edu.cn](mailto:andrew.fowlie@xjtlu.edu.cn)

‡Electronic address: [ctlu@njnu.edu.cn](mailto:ctlu@njnu.edu.cn)

§Electronic address: [Lachlan.Morris@monash.edu](mailto:Lachlan.Morris@monash.edu)

¶Electronic address: [leiwu@njnu.edu.cn](mailto:leiwu@njnu.edu.cn)

\*\*Electronic address: [211002044@njnu.edu.cn](mailto:211002044@njnu.edu.cn)

††Electronic address: [ycwu@njnu.edu.cn](mailto:ycwu@njnu.edu.cn)

percolation temperature, and that the phase transition does not complete for the low temperatures associated with a nHz signal. This finding is consistent with brief remarks in Ref. [52] and as mentioned similar to the graceful-exit problem in old inflation [53]. Secondly, even if the completion criteria is ignored or can be evaded, supercooled FOPTs may struggle to create a hierarchy between a new physics scale and the MeV scale, because the Universe reheats to the new physics scale [34]. The energy released from the phase transition reheats the surrounding plasma and the peak frequency of a SGWB we would observe today would be red-shifted [54] away from the nHz scale. The rest of this paper is structured as follows. We recapitulate the details of the supercooling model in Ref. [41] in section II and demonstrate the two difficulties in sections III A and III B, respectively. Finally, we conclude in section IV.

## II. CUBIC POTENTIAL

Following Ref. [41, 55], we construct a simple model that falls under the category of non-linearly realized electroweak symmetry. The SM Higgs doublet belongs to the coset group  $G_c = SU(2)_L \times U(1)_Y / U(1)_{EM}$  and can be expressed as

$$H(x) = \frac{r(x)}{\sqrt{2}} e^{i\theta^i(x)T^i} \begin{pmatrix} 0 \\ 1 \end{pmatrix}, \quad (1)$$

where  $i = 1 - 3$ . The SM Higgs boson is a singlet field in the SM, denoted as  $r(x) \sim (1, 1)_0$ , and the fields  $\theta^i(x)$  correspond to three would-be Goldstone bosons. The physical Higgs boson,  $h$ , is a fluctuation in  $r$  around the vacuum expectation value of electroweak symmetry breaking, that is,  $r = \langle r \rangle + h$ , where  $\langle r \rangle = v = 246 \text{ GeV}$ .

The general tree-level Higgs potential for the SM singlet field,  $r$ , can be written as

$$V_0(r) = -\frac{\mu^2}{2}r^2 + \frac{\kappa}{3}r^3 + \frac{\lambda}{4}r^4. \quad (2)$$

We add zero- and finite-temperature one-loop Coleman-Weinberg corrections to the tree-level potential, as well as daisy terms using the Parwani method to address infrared divergences,

$$V(r, T) = V_0(r) + V_{CW}(r) + V_T(r, T) + V_{\text{Daisy}}(r, T). \quad (3)$$

The formulas for  $V_{CW}(r)$ ,  $V_T(r, T)$ , and  $V_{\text{Daisy}}(r, T)$  can be found in the Appendix of Ref. [41]. There are, of course, other possible models with supercooled FOPTs, including the classic Coleman-Weinberg model [56].

The model parameters, namely  $\mu$ ,  $\kappa$ , and  $\lambda$ , are constrained by the tadpole and on-shell mass conditions,

$$\left. \frac{dV}{dr} \right|_{r=v} = 0, \quad \left. \frac{d^2V}{dr^2} \right|_{r=v} = m_h^2, \quad (4)$$

where  $m_h \simeq 125 \text{ GeV}$ . We use them to eliminate  $\mu^2$  and  $\lambda$  at the one-loop level through

$$\mu^2 = \frac{1}{2} \left( m_h^2 + \kappa v + \frac{3}{v} \left. \frac{dV_{CW}}{dr} \right|_v - \left. \frac{d^2V_{CW}}{dr^2} \right|_v \right), \quad (5a)$$

$$\lambda = \frac{1}{2v^2} \left( m_h^2 - \kappa v + \frac{1}{v} \left. \frac{dV_{CW}}{dr} \right|_v - \left. \frac{d^2V_{CW}}{dr^2} \right|_v \right). \quad (5b)$$

This requires an iterative procedure starting with the tree-level tadpole equations and repeatedly using one-loop extraction until convergence.

This leaves the cubic coupling  $\kappa$  as the only free parameter. This cubic term creates a barrier between minima in the potential and can lead to supercooling. The requirement that the potential must be bounded from below ensures that  $\lambda > 0$ . On the other hand, by convention so that  $\langle r \rangle > 0$ , we choose  $\kappa < 0$ .

In addition to the particles stated in the Appendix of Ref. [41], we add radiative corrections from all remaining quarks and the muon and tau. We account for 81 effective degrees of freedom in the one-loop and finite-temperature corrections, leaving 25.75 degrees of freedom from light particles that we treat as pure radiation. Thus we add a final term to the effective potential:

$$V_{\text{rad}}(T) = -\frac{\pi^2}{90} g'_* T^4, \quad (6)$$

where  $g'_* = 106.75 - 81 = 25.75$ .

We consider two benchmark points to highlight the challenges of fitting a nHz signal with this cubic potential:

$$\text{BP1: } \kappa = -116.81 \text{ GeV} \quad (7)$$

$$\text{BP2: } \kappa = -117.48 \text{ GeV} \quad (8)$$

BP1 resulted in the most supercooling for which the transition completes and percolation is not questionable. BP2 resulted in the most supercooling for which percolation is not questionable, though the transition does not complete. For cubic couplings even smaller than that in BP2, numerical errors in the calculation of the bounce action prevent a reliable determination of the percolation temperature. We discuss the results in the next section, with further details of the analysis left to the appendices.

## III. CHALLENGES

### A. Challenge 1 — completion

A possible strategy for achieving a peak frequency at the nHz scale is to consider a strongly supercooled phase transition, where bubble percolation is delayed to below the GeV scale. However, in many models a first-order electroweak phase transition has bubbles nucleating around the electroweak scale. There is then an extended duration of bubble growth and expansion of space. If bubbles grow too quickly compared to the expansion rate of the Universe, the bubbles will percolate too soon. Yet if bubbles grow too slowly they may never percolate due to the space between them inflating. Thus, while it is possible to tune model parameters to achieve percolation at an arbitrarily low temperature, completion of the transition becomes less likely as supercooling is increased. We define the completion temperature  $T_f$

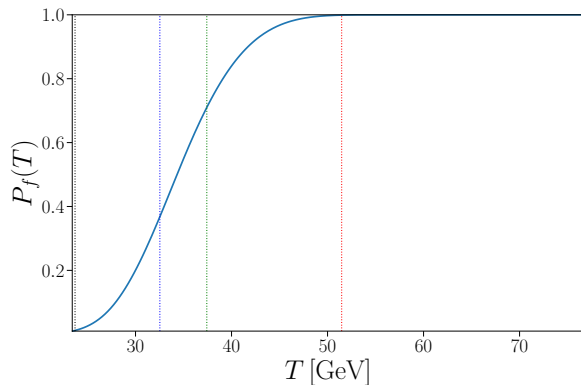


FIG. 1: The false vacuum fraction as a function of temperature for BP1 in potential with the cubic term. The vertical dotted lines are from right to left: the nucleation temperature  $T_n$  (red),  $T_p$  (green), the temperature at which  $P_f = 1/e$  (blue),  $T_f$  (black).

as the temperature for which false vacuum fraction  $P_f$  is 1%; that is,  $P_f(T_f) = 0.01$ . See appendix A 1 for details.

Consider the cubic potential. We will argue that completion is impossible if  $T_p \lesssim 1$  GeV. The same arguments apply to the models considered in Ref. [50]. In the cubic potential, strong supercooling implies a Gaussian bubble nucleation rate peaking at  $T_\Gamma \sim 50$  GeV. Percolation at say  $T_p \sim 1$  GeV and completion shortly after implies that the false vacuum fraction must drop sharply around  $T_p$ . The onset of percolation is defined by  $P_f(T_p) = 0.71$ . Because  $T_\Gamma \gg T_p$ , we must have  $P_f \approx 1$  until  $T \sim T_p$ . Otherwise the influx of nucleated bubbles would quickly percolate. However, in the cubic potential, strongly supercooling spreads out the decrease in false vacuum fraction over a large range of temperatures. This is because delayed percolation requires bubbles to slowly take over the Universe. Consequently, completion after the onset of percolation is also slow. This is demonstrated in fig. 1. We demonstrate the case of low-temperature percolation preventing completion in fig. 2.

In Ref. [8], the cubic potential is suggested as candidate model for a strongly supercooled phase transition that could explain the detected SGWB. In the original investigation [41] of detecting the cubic potential with pulsar timing arrays, the Universe was assumed to be radiation dominated. However, a more careful treatment of the energy density during strong supercooling shows that the Universe becomes vacuum dominated [52]. This leads to a period of rapid expansion that hinders bubble percolation and completion of the transition. In fact, one must check not only that  $P_f < 0.01$  eventually, but also that the physical volume of the false vacuum decreases at  $T_p$  [50, 52, 57] (again see appendix A 1 for details).

Additionally, we find that fine-tuning the cubic potential such that  $T_p \lesssim 1$  GeV is not practical given the limitations imposed by numerical errors in the bounce action calculation. Such fine-tuning was not required in the original study [41] possibly because of the assumption of radiation domination.

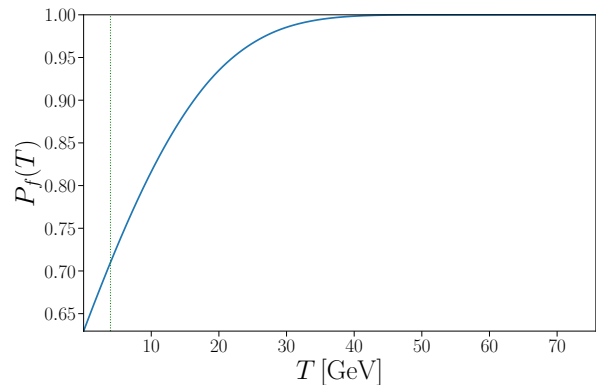


FIG. 2: The false vacuum fraction as a function of temperature for BP2.

## B. Challenge 2 – reheating

Even if the completion constraints can be avoided a second issue was recently observed [34]. Whilst supercooling could in principle be used to lower the percolation temperature  $T_p$  down to  $\mathcal{O}(100 \text{ MeV})$  or lower, the energy released from the phase transition reheats the plasma. This raises the temperature from which a SGWB would be redshifted.

Indeed, the frequency of the GWs produced during the phase transition at  $T_p$  are redshifted from the reheating temperature  $T_{\text{reh}}$  to the current time  $T \simeq 0$  (for a review, see section 6.2 of Ref. [40]). Consequently, the peak frequency today depends linearly on the reheating temperature,<sup>1</sup>

$$f_{\text{peak}|T=0} \approx 10 \text{ nHz} \left( \frac{g_*^{\text{eff}}}{100} \right)^{\frac{1}{6}} \left( \frac{T_{\text{reh}}}{100 \text{ MeV}} \right) \left( \frac{f_{\text{peak}}|_{T=T_p}}{H_*} \right) \quad (9)$$

Thus the peak frequency depends on the temperature of the FOPT and, consequently, on the mass scale of any new physics driving the phase transition. For a nHz peak frequency, temperatures of around the QCD scale or lower are expected, leading to the proposals that supercooled phase transitions can predict nHz signals by supercooling the electroweak phase transition down to around 100 MeV.

The reheating temperature is related to the percolation temperature through the approximate relation [52]

$$T_{\text{reh}} = (1 + \alpha)^{1/4} T_p. \quad (10)$$

Here the large energy released from the phase transition implies large  $\alpha$  (often referred to as the latent heat) increasing the reheating temperature. In Ref. [34], approximating the latent heat by  $\alpha \approx \Delta V / \rho_R$ , they show that in the Coleman-Weinberg model the latent heat is so large that the Universe reheats well

<sup>1</sup> There is also an implicit dependence on temperature from the degrees of freedom which can be important in slow transitions during which the Universe cools to temperatures below the EW and QCD scales. In our numerical treatment we take these effects into account.

above the percolation temperature and back to the scale of new physics.

A simple scaling argument suggests that this observation — that supercooled FOPTs reheat to the scale of new physics,  $M$  — is generic. The new physics creates a barrier between minima so we expect  $\Delta V \sim M^4$  and because the radiation energy density goes like  $T_p^4$ , we expect the latent heat may go like

$$\alpha \sim \frac{M^4}{T_p^4}. \quad (11)$$

This leads to

$$T_{\text{reh}} \sim \left( \frac{M^4}{T_p^4} \right)^{\frac{1}{4}} T_p = M. \quad (12)$$

It is possible this scaling can be avoided by fine-tuning terms to achieve  $T_{\text{reh}} \ll M$  if  $\Delta V \ll M^4$ .

This argument, however, relies on the simple approximation of the reheating temperature eq. (10) and crude dimensional analysis. We now confirm that this problem exists and is unavoidable in a careful analysis of the example model we consider. This careful treatment is general and can be used in other models. We assume that the reheating occurs instantaneously around the time of bubble percolation, and use conservation of energy so that the reheating temperature can be obtained from [50, 58]

$$\rho(\phi_f(T_p), T_p) = \rho(\phi_t(T_{\text{reh}}), T_{\text{reh}}), \quad (13)$$

where  $\phi_f$  and  $\phi_t$  are the false and true vacua respectively. In the calculation of the redshift factor for the GW spectrum we avoid the standard assumptions about radiation domination (and thermal equilibrium) by computing the redshift factor directly from the Hubble parameter, while for both the peak frequency and the Hubble parameter we carefully account for the changes in the effective number of degrees of freedom as the temperature cools. For the peak frequency we apply suppression factors from Ref. [59] to the degrees of freedom of each particle. This incorporates effects of particles decoupling from the thermal bath as the temperature drops below their respective mass.

In addition to the redshift factor we also treat the peak amplitude at the time of production with great care. For example we compute the kinetic energy available the sound wave source using the pseudotrace [60] rather than the usual approximations with assumptions regarding the bag model and the speed of sound that can easily be violated in realistic models. A full description of our treatment is given in appendices A 2 and A 3.

For BP1, the percolation temperature is  $T_p \approx 37.4$  GeV, and the transition completes and reheats the Universe to  $T_{\text{reh}} \approx 44.1$  GeV. The reheating temperature exceeds the percolation temperature due to the energy released from the supercooled phase transition, though they remain of the same order of magnitude. For BP2, however, the percolation temperature drops to  $T_p \approx 4$  GeV, whereas the reheating temperature is around 36 GeV; an order of magnitude larger.

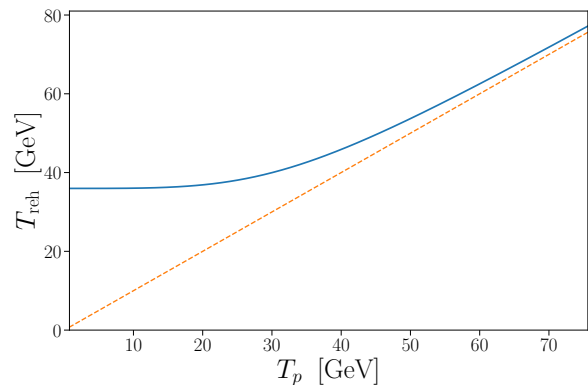


FIG. 3: Approximate reheating temperature  $T_{\text{reh}}$  against percolation temperature  $T_p$  as  $\kappa$  varied. We see that  $T_{\text{reh}} \gtrsim 40$  GeV even when  $T_p \rightarrow 0$ .

We show the approximate behavior of the reheating temperature as a function of percolation temperature in fig. 3. We find this by fixing  $T_p$  and solving eq. (13) for  $T_{\text{reh}}$  for BP2. This approximately works because the percolation temperature is extremely sensitive to  $\kappa$  and would reach  $T_p = 0$  at a finite  $\kappa$  near BP2, such that for a given percolation temperature, eq. (13) only weakly depends on  $\kappa$ . We clearly see that the reheating temperature trends towards a constant value  $T_{\text{reh}} \approx 40$  GeV for  $T_p \rightarrow 0$ . This means that the peak frequency will be much higher than one would naively expect from the percolation temperature for our benchmark points and for any point in this model with enough supercooling to have sub-GeV percolation temperatures.

### C. Gravitational Wave Spectra

We now consider the SGWB predictions. In this model we find that the bubbles mostly nucleate at temperatures around 50 GeV. We thus expect that friction from the plasma is sufficient to prevent runaway bubble walls, despite the large pressure difference. This implies that the SGWB from bubble collisions is negligible and that all the available energy goes into the fluid, resulting in a SGWB from sound waves and turbulence.

In fig. 4 we show the predicted GW spectrum for both BP1 (upper panel) — the model with the lowest percolation temperature and BP2 (lower panel) — the model with most supercooling that we can obtain in our analysis. The peak frequency for BP1 ( $3.6 \times 10^4$  nHz) is significantly higher than the peak frequency for BP2 ( $1.0 \times 10^4$  nHz). As anticipated, though, the peak frequencies do not scale linearly with the percolation temperature, which changes by an order of magnitude between these points. Instead, other factors such as the characteristic length scale (which is approximately 45 times larger in BP2) will have a large impact on the peak frequency. In both benchmarks, the GWs peak frequency is far too high to fit the nHz signal observed by the PTAs. BP1 represents the lowest peak frequency that can be obtained for realistic scenarios



in this model because for lower percolation temperatures the electroweak phase transition does not complete. This demonstrates that this model *cannot* explain the PTA signal despite various optimistic statements from the literature. BP2 shows that even if one ignores the completion requirement, the reduction in the peak frequency is not sufficient to place it in the range of the PTA signal.

Away from the peak our predicted signal does cross the uncertainty bands on the amplitude for some frequencies from the PTA signals but it does not fit most frequencies so this benchmark should also be regarded as excluded. This does however highlight the significance of considering both the peak amplitude and the peak frequency. It is also worth noting that it is the contributions from the turbulence source that dominate where they cross and this is the least well modeled of the sources and we have taken a conservative estimate of the corresponding efficiency coefficient (see the appendix).

Finally for comparison we also show in the red curves the GW prediction if one were to assume vacuum transitions instead. The bubble collisions peak at a significantly lower frequency. However, even if we were to assume a vacuum transition, which is not a realistic assumption for this model, BP1 (and the model as a whole) still cannot explain the PTA data. Finally for BP2 the peak frequency is at the right scale for a vacuum transition, however the signal is then too strong to match the observed SGWB signal. Nonetheless this does indicate that one could falsely identify a model as fitting the SGWB if the wrong assumptions are made or the completion criteria are not tested.

#### IV. CONCLUSIONS

Supercooled FOPTs are an intriguing explanation of the nHz SGWB recently observed by several PTAs, as they could connect a nHz signal to phenomenology and experiments at the electroweak scale. Indeed, they were mentioned as a possibility [1, 8]. We demonstrate, however, that there are two major difficulties in supercooled explanations. First, completion of the transition is hindered by vacuum domination. Second, the Universe typically reheats to the scale of any physics driving the transition. This redshifts any SGWB away from the nHz scale. We demonstrate that the first issue rules out the possibility of explaining the PTA signal in the supercooling model mentioned as a prototypical example in Ref. [1, 8]. We also show the second issue (reheating) can substantially shift the peak frequency and thereby weaken the GW signal in the region of interest. However we also show that this is affected by many other factors and in general the predictions for a SGWB from particle physics models require very careful treatment. We anticipate that these issues are quite generic and they should be carefully checked in any supercooled explanation.

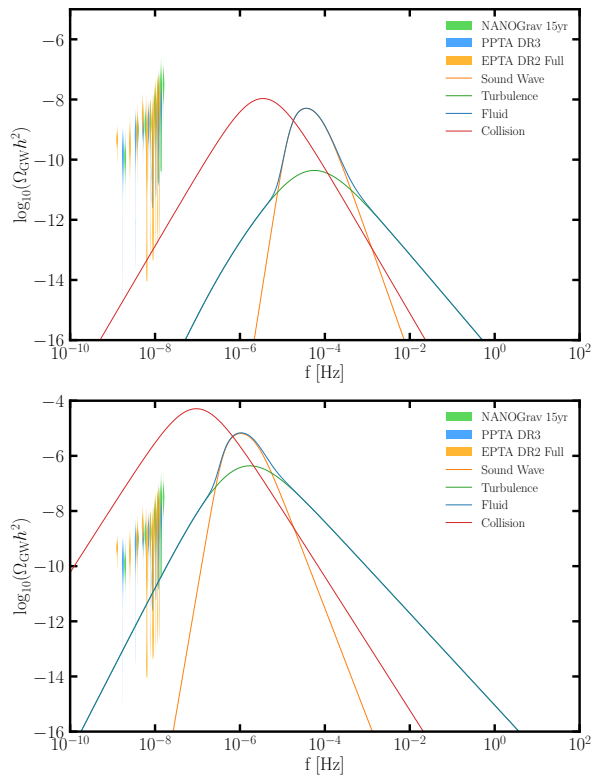


FIG. 4: The SGWB from BP1 (top panel) and BP2 (bottom panel) — the models with the most supercooling — fail to match the observations by PTA experiments. The blue curve shows the GW predictions for the case of a non-vacuum transition where we assume all the available energy goes into the fluid, which should apply to our scenarios. In this case the GWs are made up from the sum of sound wave (orange) and turbulence (green) curves. The red curve shows the GW spectra for the converse case where we assume a vacuum transition where the lack of friction leads to runaway bubble walls and bubble collisions are the sole source of GWs. Note that we do not expect this to be the case for our benchmarks here, but include it for comparison. Finally we also show the SGWB signal region from the various PTAs where the vertical spread represents the uncertainty in each frequency bin.

#### V. ACKNOWLEDGEMENTS

AF was supported by RDF-22-02-079. LM was supported by an Australian Government Research Training Program (RTP) Scholarship and a Monash Graduate Excellence Scholarship (MGES). The work of PA is supported by the National Natural Science Foundation of China (NNSFC) under grant No. 12150610460 and by the supporting fund for foreign experts grant wgxz2022021L.

#### Appendix A: Predicting gravitational waves

In this section, we summarize our calculations for the phase transition and GW spectra. First, we describe the analysis of the phase transition and then determine the relevant thermal parameters. Finally, we provide an outline of our fitting mod-

els for sound waves, turbulence, and collisions in GW spectra.

### 1. Phase transition analysis

We use PhaseTracer [61] to determine the phase structure and TransitionSolver [58] to evaluate the phase history and extract the GW signal. The particle physics model considered in this study has at most one first-order phase transition, making phase history evaluation a simple matter of analysing the single first-order phase transition. We use a modified version of CosmoTransitions [62] to calculate the bounce action during transition analysis.<sup>2</sup>

TransitionSolver tracks the false vacuum fraction [50]

$$P_f(T) = \exp\left(-\frac{4\pi}{3}v_w^3 \int_T^{T_c} dT' \frac{\Gamma(T')}{T'^4 H(T')} \left(\int_T^{T'} \frac{dT''}{H(T'')}\right)^3\right) \quad (\text{A1})$$

as a function of temperature,<sup>3</sup> where  $v_w$  is the bubble wall velocity,  $\Gamma$  is the bubble nucleation rate,  $H$  is the Hubble parameter, and  $T_c$  is the critical temperature at which the two phases have equal free-energy density. This allows us to evaluate the GW power spectrum at the onset of percolation. Percolation occurs when the false vacuum fraction falls to 71% [63–65]. Thus we define the percolation temperature,  $T_p$ , through

$$P_f(T_p) = 0.71. \quad (\text{A2})$$

This temperature will be used as the reference temperature for GW production.

The quantities in eq. (A1) are estimated as follows. The bubble wall velocity  $v_w$  is typically ultra-relativistic in the strongly supercooled scenarios we consider here, so we take  $v_w \approx 1$ . The bubble nucleation rate is estimated as [66]

$$\Gamma(T) = T^4 \left(\frac{S(T)}{2\pi}\right)^{\frac{3}{2}} \exp(-S(T)), \quad (\text{A3})$$

where  $S(T)$  is the bounce action. The Hubble parameter

$$H(T) = \sqrt{\frac{8\pi G}{3}\rho_{\text{tot}}(T)} \quad (\text{A4})$$

depends on the total energy density [50]

$$\rho_{\text{tot}}(T) = \rho_f(T) - \rho_{\text{gs}}, \quad (\text{A5})$$

and  $G = 6.7088 \times 10^{-39} \text{ GeV}^{-2}$  is Newton's gravitational constant [67]. The energy density of phase  $i$  is given by [68]

$$\rho_i(T) = V(\phi_i, T) - T \left. \frac{\partial V}{\partial T} \right|_{\phi_i(T)}, \quad (\text{A6})$$

where  $V(\phi_i, T)$  is the effective potential. The subscript  $f$  in eq. (A5) denotes the false vacuum and gs denotes the zero-temperature ground state of the potential. Finally, the transition is analysed by evaluating the false vacuum fraction eq. (A1) starting near the critical temperature and decreasing the temperature until the transition completes. We define completion to be when  $P_f(T_f) = 0.01$ , and further check that the physical volume of the false vacuum is decreasing at  $T_p$  [50, 57]; that is,

$$3 + T_p \left. \frac{d\mathcal{V}_f^{\text{ext}}}{dT} \right|_{T_p} < 0, \quad (\text{A7})$$

where  $-\mathcal{V}_f^{\text{ext}}$  is the exponent in eq. (A1). This condition was empirically determined to be the strongest completion criterion of those considered in Ref. [50], and continues to be in the models considered in this study.

### 2. Thermal parameters

The GW signal depends on several thermal parameters: the kinetic energy fraction  $K$ , the characteristic length scale  $L_*$ , the bubble wall velocity  $v_w$ , and a reference temperature  $T_*$  for GW production. We take the reference temperature to be the percolation temperature  $T_p$  because percolation necessitates bubble collisions [50]. As explained above, we take  $v_w \approx 1$  due to the strong supercooling. Specifically, we take  $v_w = 0.99995$  (or Lorentz factor  $\gamma = 100$ ) which is consistent with a supersonic detonation for the large transition strengths we find in our benchmarks.

The kinetic energy fraction is the kinetic energy available to source GWs, divided by the total energy density  $\rho_{\text{tot}}$ . We calculate this as [60]

$$K = \frac{\bar{\theta}_f(T_*) - \bar{\theta}_t(T_*)}{\rho_{\text{tot}}(T_*)} \kappa(\alpha, c_{s,f}^2, c_{s,t}^2), \quad (\text{A8})$$

where

$$\alpha = \frac{4(\bar{\theta}_f(T_*) - \bar{\theta}_t(T_*))}{3w_f} \quad (\text{A9})$$

is the transition strength parameter, and the pseudotrace  $\bar{\theta}$  is given by [69]

$$\bar{\theta}_i(T) = \frac{1}{4} \left( \rho_i(T) - \frac{p_i(T)}{c_{s,i}^2(T)} \right). \quad (\text{A10})$$

The pressure is  $p = -V$ , the enthalpy is  $w = \rho + p$ , and the speed of sound  $c_s$  is given by

$$c_{s,i}^2(T) = \left. \frac{\partial_T V}{T \partial_T^2 V} \right|_{\phi_i(T)}. \quad (\text{A11})$$

This treatment of the kinetic energy fraction corresponds to model M2 of [60]. We use the code snippet in Appendix B of [60] to calculate  $\kappa(\alpha, c_{s,f}^2, c_{s,t}^2)$ . For turbulence, we take the

<sup>2</sup> The modifications are described in Appendix F of Ref. [50]. Most important are the fixes for underflow and overflow errors.

<sup>3</sup> See Ref. [50] and Section 4 of Ref. [40] for the assumptions implicit in (A1).

efficiency coefficient to be 5% and show it merely for comparison. Modeling the efficiency of the turbulence source is still an open research problem.

We also consider a case where bubble collisions alone source GWs. In this case we ignore the sound wave and turbulence sources altogether and use  $K = \alpha/(1 + \alpha)$  for the collision source. This assumes that the efficiency for generating GWs from the bubble collisions is maximal, which we take as a limiting case. We do not calculate the friction in the cubic potential so a proper estimate of the efficiency coefficient for the collision source is not possible.

We use the mean bubble separation  $R_*$  for the characteristic length scale. We calculate  $R_*$  directly from the bubble number density,  $n_B(T)$ : [40]

$$R_*(T) = (n_B(T))^{-\frac{1}{3}} = \left( T^3 \int_T^{T_c} dT' \frac{\Gamma(T') P_f(T')}{T'^4 H(T')} \right)^{-\frac{1}{3}}. \quad (\text{A12})$$

We also incorporate the suppression factor

$$\Upsilon(\tau_{\text{sw}}) = 1 - \frac{1}{\sqrt{1 + 2H_* \tau_{\text{sw}}}}, \quad (\text{A13})$$

in our GW predictions, which arises from the finite lifetime of the sound wave source [70]. The timescale  $\tau_{\text{sw}}$  is estimated by the shock formation time  $\tau_{\text{sw}} \sim L_*/\bar{U}_f$ , where  $\bar{U}_f = \sqrt{K\rho_f/\bar{w}}$  and  $\bar{w}$  is the average enthalpy density [40].

### 3. Gravitational waves

We consider three contributions to the GW signal: bubble collisions, sound waves in the plasma, and magnetohydrodynamic turbulence in the plasma. For simplicity, we consider two scenarios: 1) non-runaway bubbles, where GWs are sourced purely by the plasma because the energy stored in bubble walls is dissipated into the plasma; and 2) runaway bubbles, where GWs are sourced purely by the energy stored in the bubble walls. We do not consider the fluid shells in this latter case. In the following, we reverse common mappings such as  $R_* = (8\pi)^{\frac{1}{3}} v_w/\beta$  and  $K = \kappa\alpha/(1 + \alpha)$  to generalise the GW fits beyond assumptions made in the original papers. This generalisation comes at the cost of further extrapolation, beyond what is already inherent in using such fits. We refer the reader to the reviews in Ref. [38–40] for further discussions on the GW fits listed below.

We use the recent GW fit for the collision source from Ref. [71]. The peak amplitude is

$$h^2 \Omega_{\text{coll},0} = 1.67 \times 10^{-5} \left[ \frac{100}{g_*} \right]^{\frac{1}{3}} \Omega_{\text{coll}}(f), \quad (\text{A14})$$

where  $\Omega_{\text{coll}}$  is the amplitude at the time of production,

$$\Omega_{\text{coll}}(f) = \left[ \frac{HR_*}{(8\pi)^{\frac{1}{3}} v_w} \right]^2 K^2 S_{\text{coll}}(f), \quad (\text{A15})$$

and the spectral shape is

$$S_{\text{coll}}(f) = \frac{A(a+b)^c}{\left[ b \left( \frac{f}{f_{p,0}} \right)^{-\frac{a}{c}} + a \left( \frac{f}{f_{p,0}} \right)^{\frac{b}{c}} \right]^c}. \quad (\text{A16})$$

The redshifted peak frequency is

$$f_{p,0} = h_* \left[ \frac{f_p}{H} \right], \quad (\text{A17})$$

where

$$h_* = 1.65 \times 10^{-5} \text{ Hz} \left( \frac{T_{\text{reh}}}{100 \text{ GeV}} \right) \left( \frac{g_*}{100} \right)^{\frac{1}{6}}. \quad (\text{A18})$$

The fit parameters  $A$ ,  $a$ ,  $b$ ,  $c$ ,  $f_p$  can be found in Table I in Ref. [71], specifically the  $T_{rr} \propto R^{-3}$  column for bubbles.

For the sound wave source, we use the GW fits in the sound shell model [72] from Refs. [73, 74]. The peak amplitude is given by

$$h^2 \Omega_{\text{sw}}(f) = 1.67 \times 10^{-5} \left( \frac{g_*}{100} \right)^{-\frac{1}{3}} 3K^2 \left( \frac{H_* R_{\text{sep}}}{c_{s,f}} \right) \times \Upsilon(\tau_{\text{sw}}) \frac{M(s, r_b, b)}{\mu_f(r_b)} \tilde{\Omega}_{\text{gw}}, \quad (\text{A19})$$

with spectral shape

$$M(s, r_b, b) = s^9 \left( \frac{1 + r_b^4}{r_b^4 + s^4} \right)^{(9-b)/4} \left( \frac{b+4}{b+4-m+ms^2} \right)^{(b+4)/2}, \quad (\text{A20})$$

where

$$m = (9r_b^4 + b) / (r_b^4 + 1), \quad (\text{A21})$$

$s = f/f_p$ ,  $r_b = f_b/f_p$ , and

$$\mu_f(r_b) = 4.78 - 6.27r_b + 3.34r_b^2. \quad (\text{A22})$$

In eq. (A19) we have used  $\tau_c \sim R_*/c_{s,f}$  for the autocorrelation timescale [39], hence the factor  $1/c_{s,f}$ . We take  $\tilde{\Omega}_{\text{gw}} = 0.01$  in accordance with Table IV of Ref. [75], and  $b = 1$ . The breaks in the power laws are governed by the mean bubble separation and the fluid shell thickness, which respectively correspond to

$$f_b = 8.9 \times 10^{-6} \text{ Hz} \left( \frac{g_*}{100} \right)^{\frac{1}{6}} \left( \frac{T_{\text{reh}}}{100 \text{ GeV}} \right) \left( \frac{8\pi}{H_* R_{\text{sep}}} \right)^{\frac{1}{3}} \left( \frac{z_p}{10} \right) \quad (\text{A23})$$

and

$$f_p = 8.9 \times 10^{-6} \text{ Hz} \left( \frac{g_*}{100} \right)^{\frac{1}{6}} \left( \frac{T_{\text{reh}}}{100 \text{ GeV}} \right) \left( \frac{8\pi}{H_* R_* \Delta_w} \right)^{\frac{1}{3}} \left( \frac{z_p}{10} \right). \quad (\text{A24})$$

The length scale for the fluid shell thickness is roughly [73]

$$R_* \Delta_w \approx R_* |v_w - c_{s,f}| / v_w, \quad (\text{A25})$$

although see Ref. [40] for further discussion. We take  $z_p = 10$  which should hold for the supersonic detonations we consider [75].

Finally, for the turbulence fit, we use the fits from Ref. [76]. The peak amplitude is proportional to

$$h^2\Omega_{\text{turb}}(f) = 3.35 \times 10^{-4} \left(\frac{g_*}{100}\right)^{-\frac{1}{3}} \left(\frac{H_* R_*}{(8\pi)^{\frac{1}{3}}}\right) (\kappa_{\text{turb}} K)^{\frac{3}{2}} S_{\text{turb}}(f), \quad (\text{A26})$$

with unnormalised spectral shape

$$S_{\text{turb}}(f) = \frac{(f/f_{\text{turb}})^3}{(1 + f/f_{\text{turb}})^{\frac{11}{3}} (1 + 8\pi f/h_*)}. \quad (\text{A27})$$

We take  $\kappa_{\text{turb}} = 0.05$  as a conservative estimate of the turbulence source in a strongly supercooled transition. The peak frequency is

$$f_{\text{turb}} = 2.7 \times 10^{-5} \text{ Hz} \left(\frac{g_*}{100}\right)^{\frac{1}{6}} \left(\frac{T_{\text{reh}}}{100\text{GeV}}\right) \left(\frac{(8\pi)^{\frac{1}{3}}}{H_* R_{\text{sep}}}\right). \quad (\text{A28})$$

- 
- [1] NANOGrav collaboration, *The NANOGrav 15-year Data Set: Evidence for a Gravitational-Wave Background*, [2306.16213](#).
- [2] H. Xu et al., *Searching for the nano-Hertz stochastic gravitational wave background with the Chinese Pulsar Timing Array Data Release I*, [2306.16216](#).
- [3] J. Antoniadis et al., *The second data release from the European Pulsar Timing Array III. Search for gravitational wave signals*, [2306.16214](#).
- [4] D.J. Reardon et al., *Search for an isotropic gravitational-wave background with the Parkes Pulsar Timing Array*, [2306.16215](#).
- [5] J.A. Casey-Clyde, C.M.F. Mingarelli, J.E. Greene, K. Pardo, M. Nañez and A.D. Goulding, *A Quasar-based Supermassive Black Hole Binary Population Model: Implications for the Gravitational Wave Background*, *Astrophys. J.* **924** (2022) 93 [[2107.11390](#)].
- [6] L.Z. Kelley, L. Blecha and L. Hernquist, *Massive Black Hole Binary Mergers in Dynamical Galactic Environments*, *Mon. Not. Roy. Astron. Soc.* **464** (2017) 3131 [[1606.01900](#)].
- [7] L.Z. Kelley, L. Blecha, L. Hernquist, A. Sesana and S.R. Taylor, *The Gravitational Wave Background from Massive Black Hole Binaries in Illustris: spectral features and time to detection with pulsar timing arrays*, *Mon. Not. Roy. Astron. Soc.* **471** (2017) 4508 [[1702.02180](#)].
- [8] NANOGrav collaboration, *The NANOGrav 15-year Data Set: Search for Signals from New Physics*, [2306.16219](#).
- [9] NANOGrav collaboration, *The NANOGrav 12.5 yr Data Set: Search for an Isotropic Stochastic Gravitational-wave Background*, *Astrophys. J. Lett.* **905** (2020) L34 [[2009.04496](#)].
- [10] NANOGrav collaboration, *Searching for Gravitational Waves from Cosmological Phase Transitions with the NANOGrav 12.5-Year Dataset*, *Phys. Rev. Lett.* **127** (2021) 251302 [[2104.13930](#)].
- [11] Z. Yi and Z.-H. Zhu, *NANOGrav signal and LIGO-Virgo primordial black holes from the Higgs field*, *JCAP* **05** (2022) 046 [[2105.01943](#)].
- [12] S. Vagnozzi, *Implications of the NANOGrav results for inflation*, *Mon. Not. Roy. Astron. Soc.* **502** (2021) L11 [[2009.13432](#)].
- [13] T.-J. Gao, *NANOGrav Signal from double-inflection-point inflation and dark matter*, [2110.00205](#).
- [14] A. Ashoorioon, K. Rezazadeh and A. Rostami, *NANOGrav signal from the end of inflation and the LIGO mass and heavier primordial black holes*, *Phys. Lett. B* **835** (2022) 137542 [[2202.01131](#)].
- [15] Y. Nakai, M. Suzuki, F. Takahashi and M. Yamada, *Gravitational Waves and Dark Radiation from Dark Phase Transition: Connecting NANOGrav Pulsar Timing Data and Hubble Tension*, *Phys. Lett. B* **816** (2021) 136238 [[2009.09754](#)].
- [16] W. Ratzinger and P. Schwaller, *Whispers from the dark side: Confronting light new physics with NANOGrav data*, *SciPost Phys.* **10** (2021) 047 [[2009.11875](#)].
- [17] S. Blasi, V. Brdar and K. Schmitz, *Has NANOGrav found first evidence for cosmic strings?*, *Phys. Rev. Lett.* **126** (2021) 041305 [[2009.06607](#)].
- [18] J. Ellis and M. Lewicki, *Cosmic String Interpretation of NANOGrav Pulsar Timing Data*, *Phys. Rev. Lett.* **126** (2021) 041304 [[2009.06555](#)].
- [19] W. Buchmuller, V. Domcke and K. Schmitz, *From NANOGrav to LIGO with metastable cosmic strings*, *Phys. Lett. B* **811** (2020) 135914 [[2009.10649](#)].
- [20] J.J. Blanco-Pillado, K.D. Olum and J.M. Wachter, *Comparison of cosmic string and superstring models to NANOGrav 12.5-year results*, *Phys. Rev. D* **103** (2021) 103512 [[2102.08194](#)].
- [21] N. Ramberg and L. Visinelli, *QCD axion and gravitational waves in light of NANOGrav results*, *Phys. Rev. D* **103** (2021) 063031 [[2012.06882](#)].
- [22] K. Inomata, M. Kawasaki, K. Mukaida and T.T. Yanagida, *NANOGrav Results and LIGO-Virgo Primordial Black Holes in Axionlike Curvaton Models*, *Phys. Rev. Lett.* **126** (2021) 131301 [[2011.01270](#)].
- [23] A.S. Sakharov, Y.N. Eroshenko and S.G. Rubin, *Looking at the NANOGrav signal through the anthropic window of axionlike particles*, *Phys. Rev. D* **104** (2021) 043005 [[2104.08750](#)].
- [24] M. Kawasaki and H. Nakatsuka, *Gravitational waves from type II axion-like curvaton model and its implication for NANOGrav result*, *JCAP* **05** (2021) 023 [[2101.11244](#)].
- [25] A. Neronov, A. Roper Pol, C. Caprini and D. Semikoz, *NANOGrav signal from magnetohydrodynamic turbulence at the QCD phase transition in the early Universe*, *Phys. Rev. D* **103** (2021) 041302 [[2009.14174](#)].
- [26] A. Addazi, Y.-F. Cai, Q. Gan, A. Marciano and K. Zeng, *NANOGrav results and dark first order phase transitions*, *Sci. China Phys. Mech. Astron.* **64** (2021) 290411 [[2009.10327](#)].
- [27] S.-L. Li, L. Shao, P. Wu and H. Yu, *NANOGrav signal from first-order confinement-deconfinement phase transition in different QCD-matter scenarios*, *Phys. Rev. D* **104** (2021) 043510 [[2101.08012](#)].
- [28] D. Borah, A. Dasgupta and S.K. Kang, *Gravitational waves from a dark U(1)D phase transition in light of NANOGrav 12.5 yr data*, *Phys. Rev. D* **104** (2021) 063501 [[2105.01007](#)].
- [29] D. Borah, A. Dasgupta and S.K. Kang, *A first order dark SU(2)<sub>D</sub> phase transition with vector dark matter in the light of NANOGrav 12.5 yr data*, *JCAP* **12** (2021) 039 [[2109.11558](#)].
- [30] K. Freese and M.W. Winkler, *Have pulsar timing arrays detected the hot big bang: Gravitational waves from strong first order phase transitions in the early Universe*, *Phys. Rev. D*



- 106** (2022) 103523 [2208.03330].
- [31] K. Freese and M.W. Winkler, *Dark matter and gravitational waves from a dark big bang*, *Phys. Rev. D* **107** (2023) 083522 [2302.11579].
- [32] Y. Bai and M. Korwar, *Cosmological constraints on first-order phase transitions*, *Phys. Rev. D* **105** (2022) 095015 [2109.14765].
- [33] T. Bringmann, P.F. Depta, T. Konstandin, K. Schmidt-Hoberg and C. Tasillo, *Does NANOGrav observe a dark sector phase transition?*, **2306.09411**.
- [34] E. Madge, E. Morgante, C.P. Ibáñez, N. Ramberg, W. Ratzinger, S. Schenk et al., *Primordial gravitational waves in the nano-Hertz regime and PTA data – towards solving the GW inverse problem*, **2306.14856**.
- [35] C. Giovanetti, M. Lisanti, H. Liu and J.T. Ruderman, *Joint Cosmic Microwave Background and Big Bang Nucleosynthesis Constraints on Light Dark Sectors with Dark Radiation*, *Phys. Rev. Lett.* **129** (2022) 021302 [2109.03246].
- [36] PLANCK collaboration, *Planck 2018 results. VI. Cosmological parameters*, *Astron. Astrophys.* **641** (2020) A6 [1807.06209].
- [37] Y. Bai and P. Schwaller, *Scale of dark QCD*, *Phys. Rev. D* **89** (2014) 063522 [1306.4676].
- [38] C. Caprini et al., *Science with the space-based interferometer eLISA. II: Gravitational waves from cosmological phase transitions*, *JCAP* **04** (2016) 001 [1512.06239].
- [39] C. Caprini et al., *Detecting gravitational waves from cosmological phase transitions with LISA: an update*, *JCAP* **03** (2020) 024 [1910.13125].
- [40] P. Athron, C. Balázs, A. Fowlie, L. Morris and L. Wu, *Cosmological phase transitions: from perturbative particle physics to gravitational waves*, **2305.02357**.
- [41] A. Kobakhidze, C. Lagger, A. Manning and J. Yue, *Gravitational waves from a supercooled electroweak phase transition and their detection with pulsar timing arrays*, *Eur. Phys. J. C* **77** (2017) 570 [1703.06552].
- [42] E. Witten, *Cosmological Consequences of a Light Higgs Boson*, *Nucl. Phys. B* **177** (1981) 477.
- [43] S. Iso, P.D. Serpico and K. Shimada, *QCD-Electroweak First-Order Phase Transition in a Supercooled Universe*, *Phys. Rev. Lett.* **119** (2017) 141301 [1704.04955].
- [44] S. Arunasalam, A. Kobakhidze, C. Lagger, S. Liang and A. Zhou, *Low temperature electroweak phase transition in the Standard Model with hidden scale invariance*, *Phys. Lett. B* **776** (2018) 48 [1709.10322].
- [45] B. von Harling and G. Servant, *QCD-induced Electroweak Phase Transition*, *JHEP* **01** (2018) 159 [1711.11554].
- [46] P. Baratella, A. Pomarol and F. Rompineve, *The Supercooled Universe*, *JHEP* **03** (2019) 100 [1812.06996].
- [47] D. Bödeker, *Remarks on the QCD-electroweak phase transition in a supercooled universe*, *Phys. Rev. D* **104** (2021) L111501 [2108.11966].
- [48] L. Sagunski, P. Schicho and D. Schmitt, *Supercool exit: Gravitational waves from QCD-triggered conformal symmetry breaking*, *Phys. Rev. D* **107** (2023) 123512 [2303.02450].
- [49] ATLAS collaboration, *Constraints on the Higgs boson self-coupling from single- and double-Higgs production with the ATLAS detector using pp collisions at  $s=13$  TeV*, *Phys. Lett. B* **843** (2023) 137745 [2211.01216].
- [50] P. Athron, C. Balázs and L. Morris, *Supercool subtleties of cosmological phase transitions*, *JCAP* **03** (2023) 006 [2212.07559].
- [51] C. Balázs, Y. Xiao, J.M. Yang and Y. Zhang, *New vacuum stability limit from cosmological history*, **2301.09283**.
- [52] J. Ellis, M. Lewicki and J.M. No, *On the Maximal Strength of a First-Order Electroweak Phase Transition and its Gravitational Wave Signal*, *JCAP* **04** (2019) 003 [1809.08242].
- [53] A.H. Guth and E.J. Weinberg, *Could the Universe Have Recovered from a Slow First Order Phase Transition?*, *Nucl. Phys. B* **212** (1983) 321.
- [54] R.-G. Cai, M. Sasaki and S.-J. Wang, *The gravitational waves from the first-order phase transition with a dimension-six operator*, *JCAP* **08** (2017) 004 [1707.03001].
- [55] A. Kobakhidze, A. Manning and J. Yue, *Gravitational waves from the phase transition of a nonlinearly realized electroweak gauge symmetry*, *Int. J. Mod. Phys. D* **26** (2017) 1750114 [1607.00883].
- [56] S.R. Coleman and E.J. Weinberg, *Radiative Corrections as the Origin of Spontaneous Symmetry Breaking*, *Phys. Rev. D* **7** (1973) 1888.
- [57] M.S. Turner, E.J. Weinberg and L.M. Widrow, *Bubble nucleation in first order inflation and other cosmological phase transitions*, *Phys. Rev. D* **46** (1992) 2384.
- [58] P. Athron, C. Balázs and L. Morris, *TransitionSolver: resolving cosmological phase histories*, in preparation (2023).
- [59] L. Husdal, *On Effective Degrees of Freedom in the Early Universe*, *Galaxies* **4** (2016) 78 [1609.04979].
- [60] F. Giese, T. Konstandin, K. Schmitz and J. Van De Vis, *Model-independent energy budget for LISA*, *JCAP* **01** (2021) 072 [2010.09744].
- [61] P. Athron, C. Balázs, A. Fowlie and Y. Zhang, *PhaseTracer: tracing cosmological phases and calculating transition properties*, *Eur. Phys. J. C* **80** (2020) 567 [2003.02859].
- [62] C.L. Wainwright, *CosmoTransitions: Computing Cosmological Phase Transition Temperatures and Bubble Profiles with Multiple Fields*, *Comput. Phys. Commun.* **183** (2012) 2006 [1109.4189].
- [63] C.D. Lorenz and R.M. Ziff, *Precise determination of the critical percolation threshold for the three-dimensional “Swiss cheese” model using a growth algorithm*, *The Journal of Chemical Physics* **114** (2001) 3659.
- [64] J. Lin and H. Chen, *Continuum percolation of porous media via random packing of overlapping cube-like particles*, *Theoretical and Applied Mechanics Letters* **8** (2018) 299.
- [65] M. Li, H. Chen and J. Lin, *Numerical study for the percolation threshold and transport properties of porous composites comprising non-centrosymmetrical superovoidal pores*, *Computer Methods in Applied Mechanics and Engineering* **361** (2020) 112815.
- [66] A.D. Linde, *Decay of the False Vacuum at Finite Temperature*, *Nucl. Phys. B* **216** (1983) 421.
- [67] J. Wu, Q. Li, J. Liu, C. Xue, S. Yang, C. Shao et al., *Progress in Precise Measurements of the Gravitational Constant*, *Annalen Phys.* **531** (2019) 1900013.
- [68] J.R. Espinosa, T. Konstandin, J.M. No and G. Servant, *Energy Budget of Cosmological First-order Phase Transitions*, *JCAP* **06** (2010) 028 [1004.4187].
- [69] F. Giese, T. Konstandin and J. van de Vis, *Model-independent energy budget of cosmological first-order phase transitions—A sound argument to go beyond the bag model*, *JCAP* **07** (2020) 057 [2004.06995].
- [70] H.-K. Guo, K. Sinha, D. Vagie and G. White, *Phase Transitions in an Expanding Universe: Stochastic Gravitational Waves in Standard and Non-Standard Histories*, *JCAP* **01** (2021) 001 [2007.08537].
- [71] M. Lewicki and V. Vaskonen, *Gravitational waves from bubble collisions and fluid motion in strongly supercooled phase transitions*, *Eur. Phys. J. C* **83** (2023) 109 [2208.11697].

- [72] M. Hindmarsh, *Sound shell model for acoustic gravitational wave production at a first-order phase transition in the early Universe*, *Phys. Rev. Lett.* **120** (2018) 071301 [[1608.04735](#)].
- [73] M. Hindmarsh and M. Hijazi, *Gravitational waves from first order cosmological phase transitions in the Sound Shell Model*, *JCAP* **12** (2019) 062 [[1909.10040](#)].
- [74] C. Gowling, M. Hindmarsh, D.C. Hooper and J. Torrado, *Reconstructing physical parameters from template gravitational wave spectra at LISA: first order phase transitions*, *JCAP* **04** (2023) 061 [[2209.13551](#)].
- [75] M. Hindmarsh, S.J. Huber, K. Rummukainen and D.J. Weir, *Shape of the acoustic gravitational wave power spectrum from a first order phase transition*, *Phys. Rev. D* **96** (2017) 103520 [[1704.05871](#)].
- [76] C. Caprini, R. Durrer and G. Servant, *The stochastic gravitational wave background from turbulence and magnetic fields generated by a first-order phase transition*, *JCAP* **12** (2009) 024 [[0909.0622](#)].